Published online 23 January 2017

Nucleic Acids Research, 2017, Vol. 45, No. 9 ***5387–5398***
doi: 10.1093/nar/gkx027

Roles of MIWI, MILI and PLD6 in small RNA regulation in mouse growing oocytes

Yuka Kabayama[1,2], Hidehiro Toh[1], Ami Katanaya[3], Takayuki Sakurai[4], Shinichiro Chuma[3], Satomi Kuramochi-Miyagawa[5], Yumiko Saga[4], Toru Nakano[5] and Hiroyuki Sasaki[1,*]

[1]Division of Epigenomics and Development, Medical Institute of Bioregulation, Kyushu University, Fukuoka 812-8582, Japan, [2]Graduate School of Medical Sciences, Kyushu University, Fukuoka 812-8582, Japan, [3]Department of Development and Differentiation, Institute for Frontier Medical Sciences, Kyoto University, Kyoto 606-8507, Japan, [4]Division of Mammalian Development, Genetic Strains Research Center, National Institute of Genetics, Mishima 411-8540, Japan and [5]Department of Pathology, Medical school and Graduate School of Frontier Biosciences, Osaka University, Suita 565-0871, Japan

Received September 07, 2016; Revised December 27, 2016; Editorial Decision January 06, 2017; Accepted January 14, 2017

ABSTRACT

The mouse PIWI-interacting RNA (piRNA) pathway produces a class of 26–30-nucleotide (nt) small RNAs and is essential for spermatogenesis and retrotransposon repression. In oocytes, however, its regulation and function are poorly understood. In the present study, we investigated the consequences of loss of piRNA-pathway components in growing oocytes. When MILI (or PIWIL2), a PIWI family member, was depleted by gene knockout, almost all piRNAs disappeared. This severe loss of piRNA was accompanied by an increase in transcripts derived from specific retrotransposons, especially IAPs. MIWI (or PIWIL1) depletion had a smaller effect. In oocytes lacking PLD6 (or ZUCCHINI or MITOPLD), a mitochondrial nuclease/phospholipase involved in piRNA biogenesis in male germ cells, the piRNA level was decreased to 50% compared to wild-type, a phenotype much milder than that in males. Since PLD6 is essential for the creation of the 5′ ends of primary piRNAs in males, the presence of mature piRNA in PLD6-depleted oocytes suggests the presence of compensating enzymes. Furthermore, we identified novel 21–23-nt small RNAs, termed spiRNAs, possessing a 10-nt complementarity with piRNAs, which were produced dependent on MILI and independent of DICER. Our study revealed the differences in the biogenesis and function of the piRNA pathway between sexes.

INTRODUCTION

PIWI-interacting RNAs (piRNAs) are small, single-strand RNAs of 26–30 nucleotides (nt) that interact with the PIWI family proteins belonging to the Argonaute superfamily (1,2). In most animals, the PIWI proteins are expressed in the gonad, and the PIWI-piRNA complexes repress retrotransposons to maintain the genomic integrity of germ cells (3). The mouse genome encodes three PIWI family proteins: MIWI (PIWIL1), MILI (PIWIL2) and MIWI2 (PIWIL4). MIWI and MILI, but not MIWI2, have RNA slicer activity essential for piRNA biogenesis and retrotransposon repression (4,5). Genetic studies have revealed that a loss-of-function mutation in any of the three *Piwi* family genes causes defects in spermatogenesis (4–8). The PIWI proteins also form complexes with Tudor-domain-containing (TDRD) proteins, which are essential for piRNA biogenesis and retrotransposon repression (9–18).

Two classes of mouse piRNA have been identified: namely, primary and secondary piRNAs. Primary piRNAs are produced from long single-strand precursor RNAs derived from genomic regions called piRNA clusters (19–25). The pathway generating primary piRNAs is not fully understood, but PLD6 (also known as ZUCCHINI (ZUC) or MITOPLD), a mitochondrial protein of the nuclease/phospholipase D family, has been proposed to act as an endonuclease generating the 5′ ends of piRNAs (26–28). Indeed, loss-of-function mutations of mouse *Pld6* cause severe defects in piRNA biogenesis and spermatogenesis (29,30). PLD6 is also proposed to possess phospholipase activity that hydrolyzes cardiolipin to generate phosphatidic acid and has been implicated in the regulation of mitochondrial morphology (30,31). Besides these functions, PLD6 is involved in the formation of nuage (also known as inter-mitochondrial cement or chromatoid body), a unique cytoplasmic structure comprising most piRNA-related proteins, as this structure is disrupted in *Pld6* mutant male germ cells (29,30). Secondary piRNAs are mostly derived from retrotransposons and produced via the so-called ping-pong cycle. The MILI-primary piRNA complexes slice

*To whom correspondence should be addressed. Tel: +81 92 642 6759; Fax: +81 92 642 6799; Email: hsasaki@bioreg.kyushu-u.ac.jp

retrotransposon-derived RNAs using the piRNA as a guide and produce both MILI-bound and MIWI2-bound secondary piRNAs in male germ cells (32). However, the ping-pong cycle is driven almost exclusively by MILI (4), consistent with the previous findings that piRNA expression is significantly decreased in *Mili*-deficient testes, but less so in *Miwi2*-deficient ones (33–35).

The mouse piRNA pathway is relatively well studied in male germ cells, but less so in oocytes, although there are abundant piRNAs in oocytes (24,25,32,36). This is partly because female mutants of the piRNA-pathway components did not show any remarkable phenotype: they were healthy and fertile (4–9,13,15–18,29,30,37–40). However, a limited study showed that, in primordial follicles from *Mili*, *Gasz* and *Mvh* mutant females, the levels of retrotransposon-derived and LTR-fusion RNAs were increased (41). This phenomenon correlated with the decreased levels of the corresponding piRNAs (41).

In this report, we studied the roles of MIWI, MILI and PLD6 proteins in the piRNA biogenesis/function in mouse oocytes using gene knockout mutants. We examined nuage formation, small RNA profiles and retrotransposon derepression in mutant oocytes and ovaries and revealed differences in the piRNA biogenesis/function between males and females. Furthermore, we identified novel small RNAs of 21–23 nt that are produced dependent on MILI and independent of DICER. Our study provides the basis for further understanding of the evolutionarily conserved piRNA system in oocytes.

MATERIALS AND METHODS

Mutant mice and collection of ovaries and oocytes

Mouse husbandry and all mouse experiments were carried out under the ethical guidelines of Kyushu University. Mice were euthanized by cervical dislocation. The production and characterization of *Miwi, Mili*, *Pld6* and *Nanos3* mutant mice and *Flag-Mili* transgenic mice have been described elsewhere (6,7,34,42,43). The *Mili* catalytic mutant mice ($Mili^{DAH}$) (5) were a generous gift from Donal O'Carroll. The floxed *Dicer* mice ($Dicer^{flox/flox}$) (44) were a generous gift from Azim Surani, Donal O'Carroll and Alexander Tarakhovsky. They were all maintained in a C57/BL6 background. The floxed *Dicer* allele was deleted in oocytes by introducing a *Zp3-cre* transgene (45). Ovaries were obtained from female mice of various developmental stages. Growing oocytes were collected from the ovaries of postnatal day 10 (P10) or P20 mice. The ovaries were treated with 1 mg/ml collagenase (Sigma-Aldrich) in M2 medium (Sigma-Aldrich) for 50 min at 37°C, 0.25% trypsin/1 mM ethylenediaminetetraacetic acid for 10 min at 37°C and 0.5% protease type XIV (Sigma-Aldrich) in M2 medium for 10 min at 37°C, and then oocytes were individually collected. Fully-grown oocytes (FGOs) were released from ovaries of 7- to 8-week-old mice by pricking with a 26G injection needle in phosphate-buffered saline and then collected using glass capillary. Each oocyte was washed and all cumulus cells were removed in a drop of M2 medium (Sigma-Aldrich) by pipetting a few times with a glass capillary tube.

Electron microscopy

P14 ovaries were de-capsulated in pre-chilled phosphate-buffered saline and fixed with 2% glutaraldehyde, 2% parafolmaldehyde in 0.1 M Sorensen's phosphate buffer (pH 7.4) for 2 h at 4°C, washed 3 times with 0.1 M sucrose/0.1 M Sorensen's phosphate buffer, post-fixed with 1% OsO4, washed with 0.1 M sucrose/0.1 M Sorensen's phosphate buffer again and then dehydrated with graded concentrations of ethanol and embedded in epoxy resin. Seventy- to 90-nm sections were placed on 150-mesh copper grids, stained with uranyl acetate followed by lead citrate and then examined using a transmission electron microscope (Hitachi H-7650).

RNA isolation, reverse transcription polymerase chain reaction (RT-PCR)

Each tissue was homogenized in TRIzol (Ambion) to isolate total RNA in accordance with the manufacturer's instruction. cDNAs were synthesized from 1 μg of total RNA using random primers and PrimeScript (TaKaRa). Total RNA from oocytes was co-precipitated with yeast tRNA, and the entire sample was used to synthesize cDNAs using random primers and SuperScript III (Invitrogen). The primers for RT-PCR are listed in Supplementary Table S1.

Western blot analysis

Each tissue was homogenized in an isotonic buffer [10 mM HEPES (pH 7.5), 0.3 M mannitol, 0.1% bovine serum albumin and Protease Inhibitor Cocktail (Nacalai Tesque)] and incubated with 0.1 mM digitonin (Wako) for 5 min on ice. After centrifugation, cleared supernatant was used for detection of MIWI and MILI. The insoluble pellet was homogenized and sonicated in a sonication buffer [50 mM Tris-HCl (pH 7.5), 150 mM NaCl, 2 mM ethylenediaminetetraacetic acid and 0.5% Tween20] for detection of PLD6. Proteins were transferred on a polyvinylidene difluoride membrane. The membrane was blocked with 3% skim milk (Nacalai Tesque) for 30–60 min at room temperature and incubated with primary antibodies diluted with CangetSignal (Toyobo) as follows: MIWI (1:500, prepared in house (antigen peptide CHREPNLSLSNRLYYL)), MILI (1:250, ab36764), PLD6 (1:100, MBL) and β-actin (1:500, Santa Cruz). The membrane was washed with Tris buffered saline with 0.05% Tween20 (pH 7.6) three times and incubated with horseradish peroxidase-conjugated secondary antibodies (1:20 000, Santa Cruz) for 1 h at room temperature. Detection of chemiluminescence was performed with Chemi-Lumi One Ultra (Nacalai Tesque) and ImageQuant LAS 4000mini (GE Healthcare).

Small RNA library construction and deep sequencing

Total RNA was prepared from P20 ovaries using TRIzol (Ambion) or AllPrep DNA/RNA/miRNA Universal Kit (Qiagen), and RNA integrity numbers were determined using an Agilent 2100 Bioanalyzer (Agilent Technologies). Small RNA libraries were prepared from 1 μg of total RNA (RNA integrity number ≥ 8) using a TruSeq Small RNA Sample Prep Kit (Illumina). Briefly, adaptor-ligated RNAs

were reverse transcribed by SuperScript III (Invitrogen), and the synthesized cDNAs were used as templates for PCR amplification (8 cycles). Amplified DNA was separated on a 6% polyacrylamide gel, and the fraction corresponding to the size range of the adaptor-ligated small RNAs was isolated from the gel. The product size was measured using a High Sensitivity DNA kit (Agilent Technologies). The yield of the small RNA library was measured by quantitative RT-PCR (qRT-PCR) using a KAPA Library Quantification Kit (KAPA Biosystems), and the library concentration was adjusted to 8 pM. A PhiX Control Kit (Illumina) was used as a spike-in control for sequencing. Single-end runs of 50–51 nt were performed on Illumina MiSeq and HiSeq 1500 platforms (Illumina).

To identify the small RNAs possessing 2′-O-methylated 3′ ends, total RNA was purified from P20 ovaries using AllPrep DNA/RNA/miRNA Universal Kit (Qiagen). The open protocol of Zamore's laboratory (http://www.umassmed.edu/zamore/resources/protocols/, small RNA sequencing) was employed for oxidation of RNAs with some modifications. Briefly, 3 μg of total RNA was treated with 25 mM sodium periodate in the presence of 150 mM borax and 150 mM boric acid (pH 8.6) for 30 min at room temperature, avoiding any light. After quenching the oxidation reaction by adding 20 μg of glycogen and sodium acetate (pH 5.2), the sample was incubated at −20°C overnight. Ethanol-precipitated RNA was washed with 80% ethanol, dried and dissolved in 5 μl of RNase-free water. Library preparation was done using a TruSeq Small RNA Sample Prep Kit (Illumina), and PCR amplification was performed for 10 cycles.

To identify small RNAs bound to MILI, P10 *Flag-Mili* ovaries were homogenized in a homogenize buffer [20 mM HEPES (pH 7.5), 150 mM NaCl, 2.5 mM $MgCl_2$, 1 mM dithiothreitol, 0.1% NP-40 and Protease Inhibitor Cocktail (Nacalai Tesque)]. After sonication and centrifugation, cleared supernatant was incubated with 10 μg of M2 FLAG antibody, preincubated with 50 μl Protein A/G PLUS-Agarose (Santa Cruz), for 2 days at 4°C. The beads were washed twice with 20 mM HEPES (pH 7.5), 150 mM NaCl and 0.05% NP-40 and twice with 20 mM HEPES (pH 7.5), 300 mM NaCl and 0.05% NP-40. RNA was extracted using TRIzol and used for small RNA library preparation with a TruSeq Small RNA Sample Prep Kit (Illumina). PCR amplification was performed for 15 cycles.

Analysis of small RNA sequence reads

Raw sequence reads were first trimmed to remove the adapter sequences. Small RNA reads of 18–34 nt were analyzed according to the flowchart shown in Supplementary Figure S1. Filtering was done using BLASTN and sequences retrieved from the miRBase (46–50) and GenBank. The mouse genome (mm10) and annotation of retrotransposons (RepeatMasker track) were downloaded from the UCSC Genome Browser (51). After mapping the unique reads to the mouse genome using Bowtie v1 (52), perfectly and uniquely matched reads were used to identify small RNA clusters. A cluster was defined as a group of at least 10 26–30-nt (putative piRNAs) or 10 21–23-nt small RNAs (putative siRNAs), where any adjacent pair was less than 2000-nt away. To identify ping-pong signatures (10-nt complementarity) in small RNAs derived from long interspersed nuclear element 1 (LINE1, L1) and intracisternal A-particle (IAP) retrotransposons, one mismatch was allowed. The L1MdTf_I consensus sequence was downloaded from the Repbase (53). The IAP (MIA14) consensus sequence was obtained from the GenBank (accession no. M17551). miRNAs were used for normalization of the piRNA population.

RNA library construction and deep sequencing

Libraries were constructed from total RNA prepared from P20 ovaries using a TruSeq Stranded Total RNA Kit with Ribo-Zero Human/Mouse/Rat (Illumina) or an NEBNext® rRNA Depletion Kit (Human/Mouse/Rat) followed by NEBNext® Ultra II DNA Library Prep Kit for Illumina (New England Biolabs). Fragmentation of RNA was performed for 5 min. PCR amplification was performed for 8 cycles. The yield of the library was measured by qRT-PCR using a KAPA Library Quantification Kit (KAPA Biosystems), and the product size was checked by electrophoresis on a 2% agarose gel. Paired-end runs of 101 nt or single-end runs of 78 nt and 108 nt were performed in rapid or high output mode on an Illumina HiSeq 1500 platform.

Analysis of RNA sequence reads

The reads were mapped to the consensus sequences of retrotransposons obtained from Repbase using Bowtie v1. The sequence of the first 50 nt of read 1 was used for mapping. Uniquely mapped reads having up to 5 mismatches were used as retrotransposon-derived RNAs for further analyses.

Data from other sources

Previously published mouse small RNA sequences from mid-sized growing oocytes (AB334800–AB349184) (25), metaphase II (MII) oocytes (ALAAA0000001–ALAAA0130942, GSE45983) (36,54) and embryonic day 16.5 (E16.5) testes (GSE20327) (34) were downloaded from the public databases and reprocessed using our pipeline.

RESULTS

Miwi, *Mili* and *Pld6* are expressed in growing oocytes

All three *Piwi* family genes and *Pld6* are known to be expressed in male germ cells (16,29,55). In developing ovaries and growing oocytes, the expression of these genes was also detected, except for *Miwi2* (16,29,41,56). To examine the expression patterns of these genes in more detail, RT-PCR was performed with RNAs from mouse ovaries, oocytes and cumulus cells collected at different developmental stages (Figure 1A). *Mili* was expressed throughout the oocyte growth (from P10 oocytes to adult FGOs), consistent with the findings from a previous report (25). *Miwi* expression was first detectable in P20 oocytes and increased in adult FGOs. *Pld6* expression was detectable at all stages and highest in P20 oocytes. *Miwi2* was undetectable. Expression of all of these genes was negligible in cumulus cells except for P10 (Figure

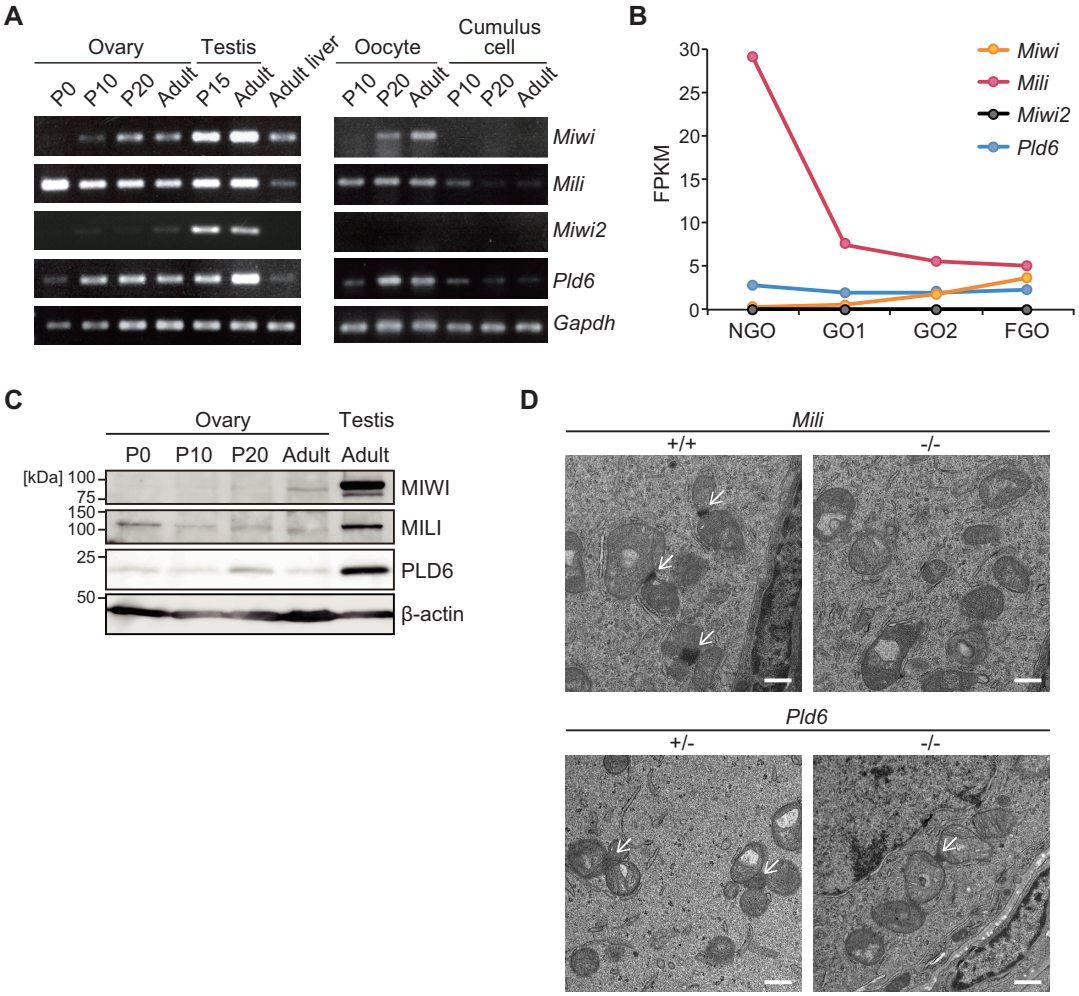

Figure 1. Expression of piRNA-related genes in wild-type oocytes and nuage formation in *Mili* and *Pld6* mutant oocytes. (**A**) Expression of the genes involved in the piRNA biogenesis/function. Growing oocytes were obtained from P10 and P20 ovaries and fully grown oocytes (FGOs) from adult ovaries. RT-PCR was performed with total RNA from the indicated tissues and cells from wild-type mice. *Gapdh* was used as a control. (**B**) Expression of the above genes in oocytes was studied using published RNA sequencing data (accession no. GSE70116) (56). FPKM, Fragments per kilobase of exon per million mapped reads; NGO, non-growing oocyte (10–40 μm); GO1, growing oocyte (25–70 μm); GO2, growing oocyte (50–70 μm); FGO, fully grown oocyte (>70 μm). (**C**) Expression of the above proteins in ovaries. Western blot analysis was performed with total proteins from ovaries and testes at indicated stages. (**D**) Electron microscopy of *Mili*$^{-/-}$ and *Pld6*$^{-/-}$ oocytes in P14 ovary sections. The control sections were from either a wild-type or a heterozygous ovary. The arrows indicate the nuage structure formed in the inter-mitochondrial spaces. The scale bars are 500 nm.

1A). Processing of the recently published data from RNA sequencing of oocytes at different stages (57) confirmed these expression patterns of the *Piwi* family genes and *Pld6* (Figure 1B). Furthermore, expression of MIWI, MILI and PLD6 proteins was detected in developing ovaries, consistent with their RNA expression patterns (Figure 1C). These results suggest that *Miwi*, *Mili* and *Pld6* are expressed during oocyte growth with a distinct developmental regulation.

Mili, but not *Pld6*, is essential for nuage formation

Many factors involved in piRNA biogenesis have been reported to be localized in the nuage, a germ-cell-specific cytoplasmic structure associated with mitochondria (58–60). The factors localized in the nuage include MIWI, MILI and PLD6, and a loss-of-function mutation of any of these factors in male germ cells disrupts nuage formation and causes derepression of retrotransposons (5,29,30,61). The nuage is also present in early-stage oocytes of primordial/primary follicles (9), and it has been reported that MILI is an important component (41). We therefore examined whether or not the nuage is affected in *Mili*$^{-/-}$ and *Pld6*$^{-/-}$ oocytes. Electron microscopy showed that the nuage disappeared from *Mili*$^{-/-}$ oocytes in P14 primary follicles (Figure 1D) as in mutant male germ cells (61). However, the nuage formation and MILI and TDRD1 localization were unaffected in *Pld6*$^{-/-}$ oocytes (Figure 1D and Supplementary Figure S1), despite the fact that *Pld6*$^{-/-}$ prospermatogonia showed diminished formation of nuage, mislocalization of its major components and dislocation of mitochondria (29). Thus, although MILI is essential for nuage formation in both male and female germ cells, PLD6 appears to be dispensable in oocytes.

Oocyte-derived piRNAs are detected by deep sequencing

The observations described above prompted us to profile the piRNAs in wild-type and mutant oocytes. We previously obtained a small RNA profile from 12 000 wild-type growing oocytes (25). To reduce the number of mice to be sacrificed and avoid labor-intensive collection of oocytes, we tested whether or not we could detect piRNAs in whole ovaries. Using the analysis flow described in Supplementary Figure S2, we obtained 200 345 retrotransposon-derived small RNA reads of 18–34 nt from 1 μg of pooled total RNA, corresponding to one-third of a whole P20 wild-type ovary (Supplementary Table S2). The size distribution of the small RNAs showed two peaks at 21–23 nt and 26–30 nt (Supplementary Figure S3A), corresponding to endogenous siRNAs (endo-siRNAs) and piRNAs, respectively (25). Consistent with the assumption that retrotransposon-derived small RNAs were from oocytes, these peaks were not observed in *Nanos3*$^{-/-}$ ovaries (Supplementary Figure S3A), which basically lacked all follicles and oocytes (42).

Genomic mapping of a small RNA fraction (731 651 reads) excluding miRNAs and degradation products of abundant non-coding RNAs revealed the presence of a total of 345 small RNA clusters in the genome of P20 ovaries (Supplementary Table S3). Among the 345 clusters, 250 predominantly produced 26–30-nt RNAs and 95 produced 21–23-nt RNAs (Supplementary Table S3), suggesting the presence of piRNA and endo-siRNA clusters. The 250 clusters predominantly producing 26–30-nt RNAs overlapped with 67% (97/144) of the piRNA clusters previously reported in growing oocytes (25). Furthermore, the small RNAs from 219 of the 250 clusters (87%) were confirmed to possess an oxidation-resistant (2′-O-methylated) 3′ end (Supplementary Figure S3B), which is a hallmark of piRNA (62–65). These small RNAs from the 250 clusters showed a tendency to possess uridine at the first position (1U) (Figure 2A), which is a feature of primary piRNA (19–22). We also investigated the 26–30-nt putative piRNA fraction derived from retrotransposons and found a bias toward adenine at position 10 (10A), as well as the bias toward 1U (Figure 2B), which are the features of secondary piRNA (23,66,67). While a similar 1U bias was observed in both cluster- and retrotransposon-derived 21–23-nt RNAs, no 10A bias was present, consistent with the assumption that these small RNAs are endo-siRNAs (Figure 2A and B). In addition to the above, a predominant 10-nt complementarity was observed between the retrotransposon-derived sense/antisense 26–30-nt putative piRNAs (Figure 2C). Together with the fact that these putative RNAs were indeed affected by *Piwi* family gene mutations (see next section), the above results indicate that there is abundant piRNA in mouse oocytes and that the so-called 'ping-pong' amplification cycle functions.

Miwi$^{-/-}$, *Mili*$^{-/-}$ and *Pld6*$^{-/-}$ ovaries show impaired piRNA biogenesis

We then performed deep sequencing of small RNAs collected from *Miwi*$^{-/-}$, *Mili*$^{-/-}$ and *Pld6*$^{-/-}$ ovaries (Supplementary Table S2). In *Miwi*$^{-/-}$ ovaries, only a small proportion of 26–30-nt piRNAs was affected, with a preferential reduction in larger piRNAs (29–30 nt) (Figure 2D), consistent with the reported binding preference of MIWI (20,21,68). In *Mili*$^{-/-}$ ovaries, both cluster- and retrotransposon-derived piRNAs were almost completely lost (Figure 2D and Supplementary Table S3), indicating that MILI is essential for either biogenesis or stability of all piRNAs in oocytes. This formally proves that these small RNAs are piRNAs. Among the retrotransposon-derived piRNAs, only those derived from short interspersed nuclear elements (SINE) were relatively well retained (48% of the wild-type) (Figure 2E and Supplementary Figure S4). However, the SINE-derived piRNAs constituted a minor fraction. The results were consistent with the observed loss of nuage in *Mili*$^{-/-}$ oocytes (Figure 1B) and a severe loss of piRNA in *Mili*$^{-/-}$ male germ cells (33,34).

In *Pld6*$^{-/-}$ ovaries, the cluster-derived piRNAs were severely affected (Figure 2D), showing that PLD6 is essential for the biogenesis of the primary piRNA in oocytes, just as in male germ cells (34) (Supplementary Figure S5). Interestingly, however, the retrotransposon-derived piRNAs were decreased to only a 54% level of that seen in wild-type ovaries (Figure 2D). This observation contrasts with the almost complete loss of retrotransposon-derived piRNAs in *Pld6*$^{-/-}$ E16.5 testes (34) (Supplementary Figure S5). Classification of the retrotransposon-derived piRNAs from *Pld6*$^{-/-}$ ovaries showed that those derived from long interspersed nuclear elements 1 (LINE1, L1) and LTR retrotransposons were decreased to levels of 11–29% (Figure 2E). However, piRNAs derived from endogenous retroviruses group K (ERVK), including those from IAP family members, were not affected (Figure 2E). Since the IAP-derived piRNAs from *Pld6*$^{-/-}$ ovaries had ping-pong signatures (Supplementary Figure S6A and B), they must have been produced in the same way as in wild-type ovaries. Again, the SINE-derived piRNA population was well retained. Thus, although PLD6 is required for the biogenesis of piRNAs from many retrotransposons, there must be other enzymes filling its role, at least for the ERVK-derived piRNAs. Lastly, any of the above mutations did not affect the profile of 21–23-nt endo-siRNAs (Supplementary Figure S6C), confirming that the piRNA and siRNA pathways are independent.

Derepression of LTR retrotransposons in *Mili*$^{-/-}$ ovaries

To examine whether or not the piRNAs have a role in retrotransposon repression in oocytes, we performed deep sequencing of total RNA. In *Mili*$^{-/-}$ovaries, several LTR retrotransposons, most predominantly IAP family members, were derepressed more than 2-fold (Figure 3). In contrast, L1 retrotransposons remained repressed (Figure 3), despite the clear loss of nuage and piRNAs. The latter finding closely correlates with our previous report (25), but contrasts with the results of limited qRT-PCR assays on P5 primordial follicles by others (41). Since a catalytic mutant of MILI showed derepression of L1 but not IAP proteins in fetal testes (4), our results suggest a sex-dependent asymmetry in retrotransposon repression by MILI. Overall, there was no correlation between the degrees of piRNA downregulation and retrotransposon derepression in *Mili*$^{-/-}$ovaries. In *Pld6*$^{-/-}$ ovaries, no detectable derepression of retrotransposons occurred (Figure 3). This again contrasts with the

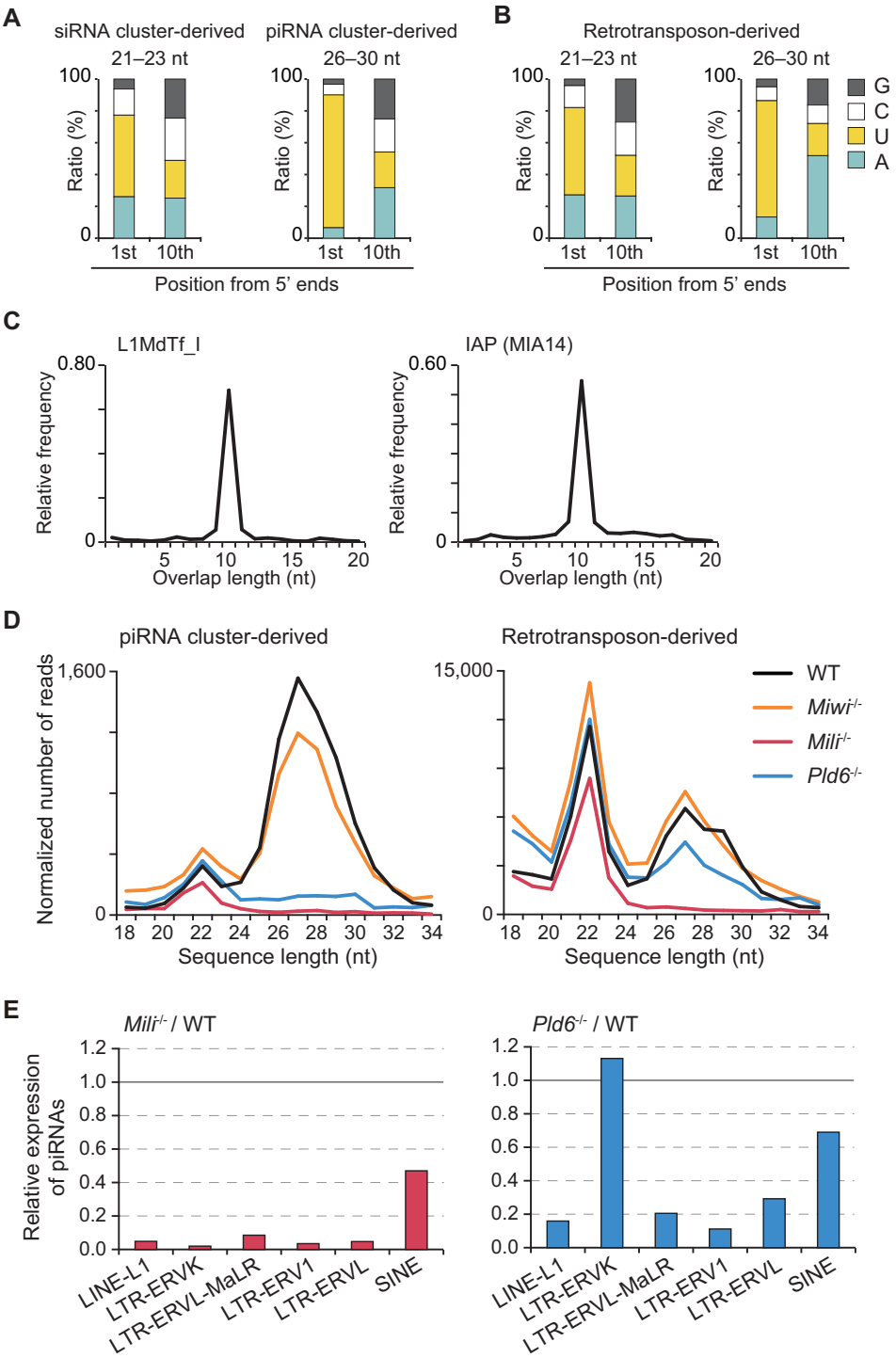

Figure 2. piRNAs profiles in wild-type and mutant oocytes. (**A**) Nucleotide compositions at the first and tenth positions of 21–23-nt RNAs from the 95 putative endo-siRNA clusters and 26–30-nt RNAs from the 250 putative piRNA clusters in wild-type ovaries. (**B**) Nucleotide compositions at the 1st and 10th positions of 21–23-nt (putative endo-siRNAs) and 26–30-nt RNAs (putative piRNAs) derived from retrotransposons in wild-type ovaries. (**C**) Relative frequencies of the lengths of complementarity detected between the 5′ portions of L1-derived 26–30-nt RNAs (putative piRNAs) and between those of intracisternal A-particle (IAP)-derived 26–30-nt RNAs in wild-type ovaries. Small RNA reads matching the consensus sequences of L1 (L1MdTf_I) and IAP (MIA14) with up to one mismatch were used. (**D**) Size distributions of the cluster- and retrotransposon-derived piRNAs in wild-type (WT), *Mili*$^{-/-}$, *Miwi*$^{-/-}$ and *Pld6*$^{-/-}$ ovaries at P20. The read number was normalized by the miRNA count in each sample. (**E**) Relative piRNA expression from individual retrotransposon families in *Mili*$^{-/-}$ and *Pld6*$^{-/-}$ ovaries.

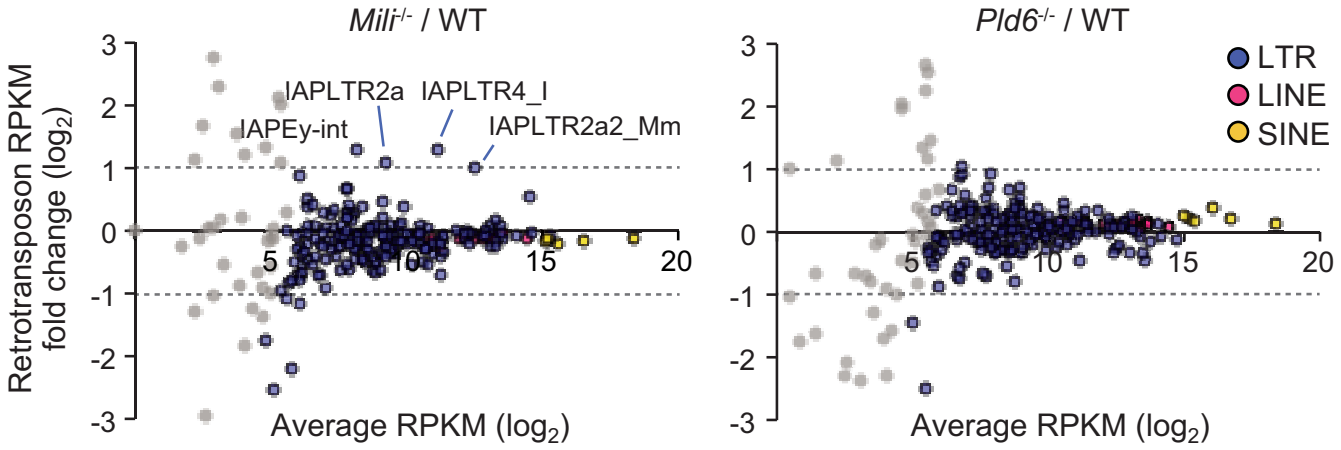

Figure 3. Role of piRNAs in retrotransposon repression in oocytes. MA plots of expression of retrotransposon-derived RNAs in *Mili*$^{-/-}$ and *Pld6*$^{-/-}$ ovaries at P20. Each spot indicates the mean (x-axis) and fold change (y-axis) of a particular retrotransposon in three biological replicates. Only those showing reads per kilobase of exons per million mapped reads (RPKM) > 50 in wild-type ovaries were colored. The dashed lines indicate twice or half of the expression level in wild-type ovaries.

findings in fetal testes where a *Pld6* mutation causes L1 and IAP derepression (29). Taken together, these findings suggest that IAP, but not L1 retrotransposons, are repressed by the piRNA pathway in mouse oocytes.

Small RNAs of 21–23 nt are also affected in *Mili*$^{-/-}$ and *Pld6*$^{-/-}$ ovaries

In the course of the above study, we found that the abundance of L1- and LTR-derived 21–23-nt RNAs, occupying a large proportion of total retrotransposon-derived 21–23-nt RNAs in wild-type ovaries (Supplementary Figure S7A), decreased in both *Mili*$^{-/-}$ and *Pld6*$^{-/-}$ ovaries (Figure 4A and Supplementary Figure S7B). This was unexpected because retrotransposon-derived 21–23-nt RNAs in oocytes are mostly endo-siRNAs (24,25), which are produced independently from piRNAs. The L1-derived 21–23-nt RNAs showed a 10-nt complementarity with L1-derived 26–30-nt piRNAs in wild-type ovaries (Figure 4B), although this was not observed between the L1-derived sense/antisense 21–23-nt RNAs. Instead, the L1-derived sense/antisense 21–23-nt RNAs showed a less prominent 19-nt complementarity (Supplementary Figure S7C) (see later). The 10-nt complementarity between the L1-derived 21–23-nt RNAs and 26–30-nt piRNAs were also found in growing oocytes and MII oocytes (Supplementary Figure S7D). These L1-derived 21–23-nt RNAs with 10-nt complementarity showed both 1U and 10A nucleotide biases (Figure 4C). In *Pld6*$^{-/-}$ ovaries, ERVK-derived 21–23-nt RNAs, including IAP-derived ones, were unaffected (Figure 4A and Supplementary Figure S7B), and a 10-nt complementarity was observed between the IAP-derived 21–23-nt RNAs and IAP-derived 26–30-nt piRNAs (Supplementary Figure S7E). However, the IAP-derived 21–23-nt RNAs decreased along with the IAP-derived piRNAs in *Mili*$^{-/-}$ ovaries (Supplementary Figure S7B), suggesting that the biogenesis of the 21–23-nt RNAs is closely related to that of 26–30-nt piRNAs.

To examine whether or not the biogenesis of L1-and IAP-derived 21–23-nt RNAs involves DICER (24,25), small RNAs from ovaries of oocyte-specific *Dicer* knockout mice (*Dicer*$^{flox/flox}$; *Zp3-cre*), referred to as *Dicer*^{CKO}, were sequenced. The *Dicer*^{CKO} mutation abolishes both somatic and oocyte-specific DICER isoforms (44). While non-retrotranposon 21–23-nt RNAs (mostly from endo-siRNA clusters) were completely lost in *Dicer*^{CKO} ovaries, a fraction of retrotransposon-derived 21–23-nt RNAs was still present (Figure 4D and Supplementary Table S3). In contrast and as expected, both cluster- and retrotransposon-derived 26–30-nt piRNAs were unaffected in this mutant (Figure 4D and Supplementary Table S3). Among the DICER-independent 21–23-nt RNAs, there were L1-derived RNAs showing a 10-nt complementarity with L1-derived 26–30-nt piRNAs (Figure 4E). However, the L1-derived 21–23-nt RNAs did not possess an oxidation-resistant 3′ end (Supplementary Figure S8), a feature of canonical piRNA.

Interestingly, the L1-derived DICER-independent 21–23-nt RNAs showed a 19-nt complementarity between themselves (Supplementary Figure S7C), a well-defined 5′ end and a short 3′ overhang of 2–4 nt, which are the features of the products of RNase III-type enzymes, including DICER (69–71) (Supplementary Figure S7F). Furthermore, some of these RNAs showed, in addition to the 10-nt complementarity with 26–30-nt piRNAs, a 19-nt complementarity with 21–23-nt RNAs (Supplementary Figure S7F). These results suggest that the biogenesis of DICER-independent 21–23-nt RNAs in oocytes involves the piRNA pathway components, but in a non-canonical way.

Novel small RNAs are bound to MILI and produced dependent on its slicer activity

We previously reported that RNAs smaller than 24 nt are bound by MILI in P8 ovaries (25). Of the 313 MILI-bound, retrotransposon-derived small RNA reads of 21–23 nt, 73 and 67 reads were derived from L1s and IAPs, respectively. However, since the number of sequenced MILI-bound 21–23-nt RNAs was too small for in-depth analyses, we performed immunoprecipitation in P10 *Flag-Mili* ovaries (43) using anti-FLAG antibody and sequenced the MILI-bound

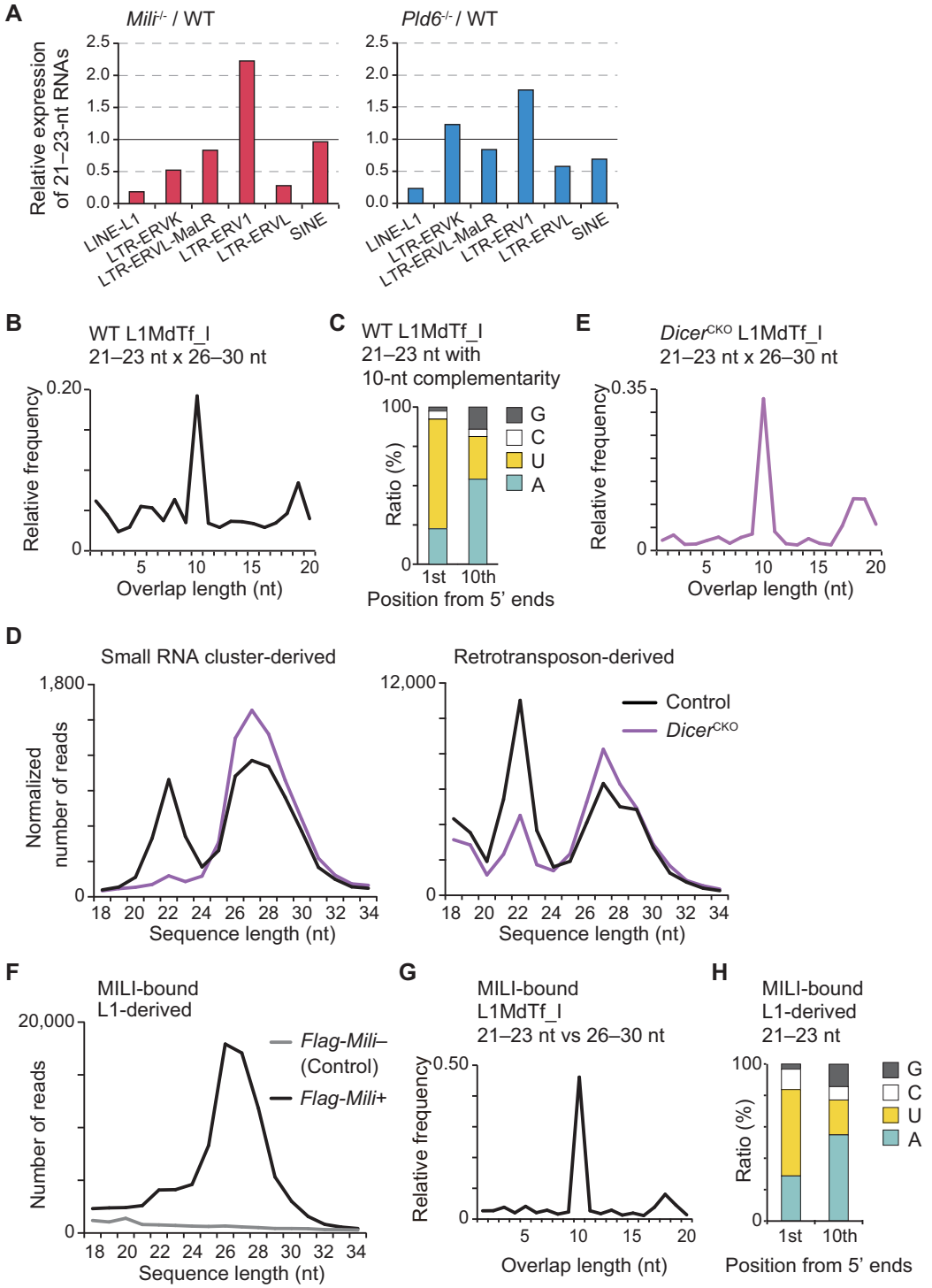

Figure 4. A class of 21–23-nt RNAs produced via the piRNA pathway, not via the endo-siRNA pathway. (**A**) Relative expression of 21–23-nt small RNAs derived from individual retrotransposon families in *Mili*$^{-/-}$ and *Pld6*$^{-/-}$ ovaries. (**B**) Relative frequencies of complementarity lengths between the 5′ portions of L1-derived 21–23-nt RNAs and those of 26–30-nt piRNAs in wild-type ovaries at P20. Small RNA reads matching the L1MdTf_I consensus sequences were selected, allowing for one mismatch and then used. (**C**) Nucleotide compositions at the first and tenth positions of L1-derived 21–23-nt RNAs showing 10-nt complementarity with L1-derived 26–30-nt piRNAs. Small RNA reads matching the L1MdTf_I consensus sequences were selected, allowing for one mismatch and then used. (**D**) Size distributions of cluster-derived (left) and retrotransposon-derived (right) small RNAs expressed in control (*Dicer*$^{flox/+}$, *Zp3-cre*$^{+}$) and *Dicer*^{CKO} ovaries. The read number was normalized by the miRNA count in each sample. (**E**) Relative frequencies of complementarity lengths between the 5′ portions of L1-derived 21–23-nt RNAs and those of 26–30-nt piRNAs expressed in P20 *Dicer*^{CKO} ovaries. Small RNA reads matching the L1MdTf_I consensus sequences with up to one mismatch were used. (**F**) Size distributions of L1-derived small RNAs bound to MILI protein in P10 ovaries. (**G**) Relative frequencies of complementarity lengths between the 5′ portions of L1-derived 21–23-nt RNAs and those of 26–30-nt piRNAs bound to MILI protein. Small RNA reads matching the L1MdTf_I consensus sequence with up to one mismatch were used. (**H**) Nucleotide compositions at the 1st and 10th positions of L1-derived 21–23-nt RNAs bound to MILI protein.

small RNAs (Figure 4F). In addition to the canonical 26–30-nt piRNAs, we obtained sequence reads of 37 272 retrotransposon-derived 21–23-nt RNAs, of which 10 786 and 4748 were from L1s and IAPs, respectively. The MILI-bound, L1MdTf_I-derived 21–23-nt RNAs clearly showed 10-nt complementarity with the MILI-bound 26–30-nt piRNAs (Figure 4G) and also both 1U and 10A nucleotide biases (Figure 4H). To examine whether biogenesis of these 21–23-nt RNAs requires the slicer activity of MILI, we sequenced small RNAs from the ovaries of *Mili*^{DAH} slicer mutant mice (5). It was found that the biogenesis of L1-derived 21–23-nt RNAs was greatly affected in *Mili*^{DAH} ovaries, together with 26–30-nt piRNAs (Supplementary Figure S9A). Furthermore, the 10-nt complementarity (ping-pong signature) between L1MdTf_I-derived 21–23-nt RNAs and 26–30-nt piRNAs became undetectable in *Mili*^{DAH} ovaries (Supplementary Figure S9B). These results indicate that the ping-pong cycle driven by the MILI slicer activity is involved in the biogenesis of the 21–23-nt RNA class. We wish to term these 21–23-nt RNAs 'short PIWI-interacting RNA' or 'spiRNA'.

DISCUSSION

In this study, we examined the roles of three major piRNA-pathway components—MIWI, MILI and PLD6—in the piRNA biogenesis/function in mouse oocytes. MIWI2, an important component of the piRNA pathway in male germ cells, was excluded from our study, since its expression was negligible throughout oocyte development (Figure 1). By small RNA profiling of mutant oocytes using deep sequencing, we revealed that all three components have a role in piRNA biogenesis in oocytes (Figure 2). Thus, the PIWI family members and PLD6 are shared between the piRNA pathways of male and female germ cells, except for MIWI2. We also obtained clear evidence that the so-called ping-pong cycle operates in oocytes as in male germ cells (Figure 2). However, we noted the following differences in the piRNA biogenesis/function between male and females.

First, in addition to the lack of MIWI2 in oocytes, the contribution of MIWI to piRNA biogenesis appears to be much smaller in oocytes than in male germ cells, although MIWI is a key player in piRNA biogenesis in male germ cells (5,68,72). Instead, the contribution of MILI is much more predominant, as its knockout mutation caused almost a complete loss of piRNAs (Figure 2), a phenotype much stronger than that in male germ cells. One possible reason for this is the much lower expression of MIWI protein than MILI protein in non-growing oocytes, growing oocytes and FGOs (25). Consistent with the observed protein levels, our RT-PCR and published RNA sequencing data (57) showed a lower expression of *Miwi* than *Mili* in growing oocytes, although their expression appears to be comparable in adult FGOs (Figure 1).

Second, we found that PLD6 is not the only enzyme that processes piRNA precursors for the creation of the 5′ ends in oocytes. Based on the small RNA profile in *Pld6* mutant ovaries (Figure 2), we speculate that there must be at least one other enzyme that processes retrotransposon-derived piRNA precursors, especially those derived from ERVK family members. Consistent with the presence of these piRNAs in *Pld6* mutant ovaries, the mutant oocytes possess appropriately formed nuage structures (Figure 1). This is surprising, because PLD6 has been shown to be essential for proper mitochondrial localization, nuage formation and production of almost all piRNAs in male germ cells (29–31). Since five other members are known to be present in the mouse PLD family, we are currently examining these PLD proteins for endonuclease activity.

Third, in contrast to the crucial role of the piRNA pathway in retrotransposon repression in male germ cells, *Mili* and *Pld6* mutations caused only limited derepression (more than 2-fold) of certain families of LTR retrotransposons (mostly IAPs) in P20 ovaries (Figure 3). In a previous report, however, the same *Mili* mutation derepressed not only IAPs, but also other LTR retrotransposons, L1s and SINEs in P5 primordial follicles (41): the discrepancy could arise from the differences in material, developmental stage, or both. Disruptions of other piRNA-pathway genes, such as *Mvh*, *Gasz* and *Mael*, also cause derepression of retrotransposons other than IAPs in primordial follicles (41) and fetal oocytes (73). The developmental regulation of individual retrotransposons by the piRNA pathway is an important issue to be addressed in future studies. All female mutants of the piRNA-pathway-component genes studied so far, including the *Mili* and *Pld6* mutants, are known to be fertile. However, a recent study on *Mael* mutant females showed a decreased number of primordial follicles in adult ovary, resulting in a loss of folliculogenesis a year later (73). Since *Mili* expression can be detected as early as E13.5 in wild-type ovaries (16), it will be interesting to examine whether or not *Mili* mutant females also have a shortened reproductive lifespan.

Lastly, we discovered a class of 21–23-nt RNAs that are derived from retrotransposons and produced dependent on the piRNA-pathway components (MILI and PLD6), but independent of the canonical siRNA-pathway component (DICER) (Figure 4). We termed these RNAs spiRNAs (for short PIWI-interacting RNAs). Despite their smaller size, spiRNAs have the sequence features of piRNAs that are amplified via the ping-pong cycle. Indeed, spiRNAs were bound by MILI (Figure 4) and produced dependent on its slicer activity (Supplementary Figure S9). In *Drosophila*, similar 21-nt RNAs have been observed among the piRNAs derived from a particular piRNA cluster (42AB) (74), which is composed of different LTR and LINE retrotransposons (65). In addition, it appears that small RNAs of about 21 nt derived from telomeric retrotransposons are affected in a piRNA-pathway mutant, *ago3* (75). Similar 19–22-nt RNAs are significantly decreased in other *Drosophila* mutants, *armi* and *aub,* as well (76). Despite all of the above, we found that spiRNAs in mouse oocytes do not possess the 2′-O-methyl modification at their 3′ ends, a hallmark of mature piRNAs. Further studies are needed to elucidate the precise mechanism of spiRNA biogenesis.

In summary, our study revealed some interesting differences in the biogenesis and function of the piRNA pathway between male and female germ cells. Our data should provide a firm basis and a better understanding of the evolutionarily conserved piRNA system in mammalian oocytes.

ACCESSION NUMBER

The sequence data in this study have been deposited in the DDBJ Sequence Read Archive under accession number DRA004523.

SUPPLEMENTARY DATA

Supplementary Data are available at NAR Online.

ACKNOWLEDGEMENTS

The authors thank Yasushi Totoki, Toshiaki Watanabe, Hatsune Chiba, Tomoko Ichiyanagi, Kenji Ichiyanagi, Yufeng Li, Kei Fukuda, Kenjiro Shirane, Naoki Kubo, Kyohei Hori, Wan Kin Au Yeung, Hiroaki Oishi and Kota Inoue for their comments and discussion on our experiments and sequence analyses. The authors thank Miho Miyake, Tomomi Akinaga, Junko Oishi, Motoko Unoki and Masato Tanaka (Kyushu University) for their technical assistance. The authors also thank Dónal O'Carroll (University of Edinburgh) for *Mili*^{DAH} mice and Dónal O'Carroll (University of Edinburgh), Azim Surani (University of Cambridge), Marianne Labriola, Cherise T. Bernard and Alexander Tarakhovsky (Rockefeller University) for *Dicer*$^{flox/flox}$ mice.

FUNDING

Grants-in-Aid for Scientific Research on Innovative Areas from JSPS to H.S. [JP25112010 to H.S., in part] and S.C. [JP25112004 to S.C., in part]. Funding for open access charge: Grants-in-Aid for Scientific Research on Innovative Areas from JSPS to H.S. [JP25112010 to H.S., in part].
Conflict of interest statement. None declared.

REFERENCES

1. Kim,V.N., Han,J. and Siomi,M.C. (2009) Biogenesis of small RNAs in animals. *Nat. Rev. Mol. Cell Biol.*, **10**, 126–139.
2. Siomi,M.C., Sato,K., Pezic,D. and Aravin,A.A. (2011) PIWI-interacting small RNAs: the vanguard of genome defence. *Nat. Rev. Mol. Cell Biol.*, **12**, 246–258.
3. Luteijn,M.J. and Ketting,R.F. (2013) PIWI-interacting RNAs: from generation to transgenerational epigenetics. *Nat. Rev. Genet.*, **14**, 523–534.
4. Reuter,M., Berninger,P., Chuma,S., Shah,H., Hosokawa,M., Funaya,C., Antony,C., Sachidanandam,R. and Pillai,R.S. (2011) Miwi catalysis is required for piRNA amplification-independent LINE1 transposon silencing. *Nature*, **480**, 264–267.
5. De Fazio,S., Bartonicek,N., Di Giacomo,M., Abreu-Goodger,C., Sankar,A., Funaya,C., Antony,C., Moreira,P.N., Enright,A.J. and O'Carroll,D. (2011) The endonuclease activity of Mili fuels piRNA amplification that silences LINE1 elements. *Nature*, **480**, 259–263.
6. Deng,W. and Lin,H. (2002) miwi, a murine homolog of piwi, encodes a cytoplasmic protein essential for spermatogenesis. *Dev. Cell*, **2**, 819–830.
7. Kuramochi-Miyagawa,S., Kimura,T., Ijiri,T.W., Isobe,T., Asada,N., Fujita,Y., Ikawa,M., Iwai,N., Okabe,M., Deng,W. *et al.* (2004) Mili, a mammalian member of piwi family gene, is essential for spermatogenesis. *Development*, **131**, 839–849.
8. Carmell,M.A., Girard,A., van de Kant,H.J., Bourc'his,D., Bestor,T.H., de Rooij,D.G. and Hannon,G.J. (2007) MIWI2 is essential for spermatogenesis and repression of transposons in the mouse male germline. *Dev. Cell*, **12**, 503–514.
9. Chuma,S., Hosokawa,M., Kitamura,K., Kasai,S., Fujioka,M., Hiyoshi,M., Takamune,K., Noce,T. and Nakatsuji,N. (2006) Tdrd1/Mtr-1, a tudor-related gene, is essential for male germ-cell differentiation and nuage/germinal granule formation in mice. *Proc. Natl. Acad. Sci. U.S.A.*, **103**, 15894–15899.
10. Chen,C., Jin,J., James,D.A., Adams-Cioaba,M.A., Park,J.G., Guo,Y., Tenaglia,E., Xu,C., Gish,G., Min,J. *et al.* (2009) Mouse Piwi interactome identifies binding mechanism of Tdrkh Tudor domain to arginine methylated Miwi. *Proc. Natl. Acad. Sci. U.S.A.*, **106**, 20336–20341.
11. Kojima,K., Kuramochi-Miyagawa,S., Chuma,S., Tanaka,T., Nakatsuji,N., Kimura,T. and Nakano,T. (2009) Associations between PIWI proteins and TDRD1/MTR-1 are critical for integrated subcellular localization in murine male germ cells. *Genes Cells*, **14**, 1155–1165.
12. Reuter,M., Chuma,S., Tanaka,T., Franz,T., Stark,A. and Pillai,R.S. (2009) Loss of the Mili-interacting Tudor domain-containing protein-1 activates transposons and alters the Mili-associated small RNA profile. *Nat. Struct. Mol. Biol.*, **16**, 639–646.
13. Shoji,M., Tanaka,T., Hosokawa,M., Reuter,M., Stark,A., Kato,Y., Kondoh,G., Okawa,K., Chujo,T., Suzuki,T. *et al.* (2009) The TDRD9-MIWI2 complex is essential for piRNA-mediated retrotransposon silencing in the mouse male germline. *Dev. Cell*, **17**, 775–787.
14. Vagin,V.V., Wohlschlegel,J., Qu,J., Jonsson,Z., Huang,X., Chuma,S., Girard,A., Sachidanandam,R., Hannon,G.J. and Aravin,A.A. (2009) Proteomic analysis of murine Piwi proteins reveals a role for arginine methylation in specifying interaction with Tudor family members. *Genes Dev.*, **23**, 1749–1762.
15. Tanaka,T., Hosokawa,M., Vagin,V.V., Reuter,M., Hayashi,E., Mochizuki,A.L., Kitamura,K., Yamanaka,H., Kondoh,G., Okawa,K. *et al.* (2011) Tudor domain containing 7 (Tdrd7) is essential for dynamic ribonucleoprotein (RNP) remodeling of chromatoid bodies during spermatogenesis. *Proc. Natl. Acad. Sci. U.S.A.*, **108**, 10579–10584.
16. Yabuta,Y., Ohta,H., Abe,T., Kurimoto,K., Chuma,S. and Saitou,M. (2011) TDRD5 is required for retrotransposon silencing, chromatoid body assembly, and spermiogenesis in mice. *J. Cell Biol.*, **192**, 781–795.
17. Pandey,R.R., Tokuzawa,Y., Yang,Z., Hayashi,E., Ichisaka,T., Kajita,S., Asano,Y., Kunieda,T., Sachidanandam,R., Chuma,S. *et al.* (2013) Tudor domain containing 12 (TDRD12) is essential for secondary PIWI interacting RNA biogenesis in mice. *Proc. Natl. Acad. Sci. U.S.A.*, **110**, 16492–16497.
18. Saxe,J.P., Chen,M., Zhao,H. and Lin,H. (2013) Tdrkh is essential for spermatogenesis and participates in primary piRNA biogenesis in the germline. *EMBO J.*, **32**, 1869–1885.
19. Aravin,A., Gaidatzis,D., Pfeffer,S., Lagos-Quintana,M., Landgraf,P., Iovino,N., Morris,P., Brownstein,M.J., Kuramochi-Miyagawa,S., Nakano,T. *et al.* (2006) A novel class of small RNAs bind to MILI protein in mouse testes. *Nature*, **442**, 203–207.
20. Girard,A., Sachidanandam,R., Hannon,G.J. and Carmell,M.A. (2006) A germline-specific class of small RNAs binds mammalian Piwi proteins. *Nature*, **442**, 199–202.
21. Grivna,S.T., Beyret,E., Wang,Z. and Lin,H. (2006) A novel class of small RNAs in mouse spermatogenic cells. *Genes Dev.*, **20**, 1709–1714.
22. Watanabe,T., Takeda,A., Tsukiyama,T., Mise,K., Okuno,T., Sasaki,H., Minami,N. and Imai,H. (2006) Identification and characterization of two novel classes of small RNAs in the mouse germline: retrotransposon-derived siRNAs in oocytes and germline small RNAs in testes. *Genes Dev.*, **20**, 1732–1743.
23. Aravin,A.A., Sachidanandam,R., Girard,A., Fejes-Toth,K. and Hannon,G.J. (2007) Developmentally regulated piRNA clusters implicate MILI in transposon control. *Science*, **316**, 744–747.
24. Tam,O.H., Aravin,A.A., Stein,P., Girard,A., Murchison,E.P., Cheloufi,S., Hodges,E., Anger,M., Sachidanandam,R., Schultz,R.M. *et al.* (2008) Pseudogene-derived small interfering RNAs regulate gene expression in mouse oocytes. *Nature*, **453**, 534–538.
25. Watanabe,T., Totoki,Y., Toyoda,A., Kaneda,M., Kuramochi-Miyagawa,S., Obata,Y., Chiba,H., Kohara,Y., Kono,T., Nakano,T. *et al.* (2008) Endogenous siRNAs from naturally formed dsRNAs regulate transcripts in mouse oocytes. *Nature*, **453**, 539–543.

26. Ipsaro,J.J., Haase,A.D., Knott,S.R., Joshua-Tor,L. and Hannon,G.J. (2012) The structural biochemistry of Zucchini implicates it as a nuclease in piRNA biogenesis. *Nature*, **491**, 279–283.
27. Nishimasu,H., Ishizu,H., Saito,K., Fukuhara,S., Kamatani,M.K., Bonnefond,L., Matsumoto,N., Nishizawa,T., Nakanaga,K., Aoki,J. *et al.* (2012) Structure and function of Zucchini endoribonuclease in piRNA biogenesis. *Nature*, **491**, 284–287.
28. Voigt,F., Reuter,M., Kasaruho,A., Schulz,E.C., Pillai,R.S. and Barabas,O. (2012) Crystal structure of the primary piRNA biogenesis factor Zucchini reveals similarity to the bacterial PLD endonuclease Nuc. *RNA*, **18**, 2128–2134.
29. Watanabe,T., Chuma,S., Yamamoto,Y., Kuramochi-Miyagawa,S., Totoki,Y., Toyoda,A., Hoki,Y., Fujiyama,A., Shibata,T., Sado,T. *et al.* (2011) MITOPLD is a mitochondrial protein essential for nuage formation and piRNA biogenesis in the mouse germline. *Dev. Cell*, **20**, 364–375.
30. Huang,H., Gao,Q., Peng,X., Choi,S.Y., Sarma,K., Ren,H., Morris,A.J. and Frohman,M.A. (2011) piRNA-associated germline nuage formation and spermatogenesis require MitoPLD profusogenic mitochondrial-surface lipid signaling. *Dev. Cell*, **20**, 376–387.
31. Choi,S.Y., Huang,P., Jenkins,G.M., Chan,D.C., Schiller,J. and Frohman,M.A. (2006) A common lipid links Mfn-mediated mitochondrial fusion and SNARE-regulated exocytosis. *Nat. Cell Biol.*, **8**, 1255–1262.
32. Aravin,A.A., Sachidanandam,R., Bourc'his,D., Schaefer,C., Pezic,D., Toth,K.F., Bestor,T. and Hannon,G.J. (2008) A piRNA pathway primed by individual transposons is linked to de novo DNA methylation in mice. *Mol. Cell*, **31**, 785–799.
33. Kuramochi-Miyagawa,S., Watanabe,T., Gotoh,K., Totoki,Y., Toyoda,A., Ikawa,M., Asada,N., Kojima,K., Yamaguchi,Y., Ijiri,T.W. *et al.* (2008) DNA methylation of retrotransposon genes is regulated by Piwi family members MILI and MIWI2 in murine fetal testes. *Genes Dev.*, **22**, 908–917.
34. Watanabe,T., Tomizawa,S., Mitsuya,K., Totoki,Y., Yamamoto,Y., Kuramochi-Miyagawa,S., Iida,N., Hoki,Y., Murphy,P.J., Toyoda,A. *et al.* (2011) Role for piRNAs and noncoding RNA in de novo DNA methylation of the imprinted mouse Rasgrf1 locus. *Science*, **332**, 848–852.
35. Manakov,S.A., Pezic,D., Marinov,G.K., Pastor,W.A., Sachidanandam,R. and Aravin,A.A. (2015) MIWI2 and MILI have differential effects on piRNA biogenesis and DNA methylation. *Cell Rep.*, **12**, 1234–1243.
36. Ohnishi,Y., Totoki,Y., Toyoda,A., Watanabe,T., Yamamoto,Y., Tokunaga,K., Sakaki,Y., Sasaki,H. and Hohjoh,H. (2010) Small RNA class transition from siRNA/piRNA to miRNA during pre-implantation mouse development. *Nucleic Acids Res.*, **38**, 5141–5151.
37. Tanaka,S.S., Toyooka,Y., Akasu,R., Katoh-Fukui,Y., Nakahara,Y., Suzuki,R., Yokoyama,M. and Noce,T. (2000) The mouse homolog of Drosophila Vasa is required for the development of male germ cells. *Genes Dev.*, **14**, 841–853.
38. Ma,L., Buchold,G.M., Greenbaum,M.P., Roy,A., Burns,K.H., Zhu,H., Han,D.Y., Harris,R.A., Coarfa,C., Gunaratne,P.H. *et al.* (2009) GASZ is essential for male meiosis and suppression of retrotransposon expression in the male germline. *PLoS Genet.*, **5**, e1000635.
39. Zheng,K., Xiol,J., Reuter,M., Eckardt,S., Leu,N.A., McLaughlin,K.J., Stark,A., Sachidanandam,R., Pillai,R.S. and Wang,P.J. (2010) Mouse MOV10L1 associates with Piwi proteins and is an essential component of the Piwi-interacting RNA (piRNA) pathway. *Proc. Natl. Acad. Sci. U.S.A.*, **107**, 11841–11846.
40. Frost,R.J., Hamra,F.K., Richardson,J.A., Qi,X., Bassel-Duby,R. and Olson,E.N. (2010) MOV10L1 is necessary for protection of spermatocytes against retrotransposons by Piwi-interacting RNAs. *Proc. Natl. Acad. Sci. U.S.A.*, **107**, 11847–11852.
41. Lim,A.K., Lorthongpanich,C., Chew,T.G., Tan,C.W., Shue,Y.T., Balu,S., Gounko,N., Kuramochi-Miyagawa,S., Matzuk,M.M., Chuma,S. *et al.* (2013) The nuage mediates retrotransposon silencing in mouse primordial ovarian follicles. *Development*, **140**, 3819–3825.
42. Tsuda,M., Sasaoka,Y., Kiso,M., Abe,K., Haraguchi,S., Kobayashi,S. and Saga,Y. (2003) Conserved role of nanos proteins in germ cell development. *Science*, **301**, 1239–1241.
43. Yamamoto,Y., Watanabe,T., Hoki,Y., Shirane,K., Li,Y., Ichiiyanagi,K., Kuramochi-Miyagawa,S., Toyoda,A., Fujiyama,A., Oginuma,M. *et al.* (2013) Targeted gene silencing in mouse germ cells by insertion of a homologous DNA into a piRNA generating locus. *Genome Res.*, **23**, 292–299.
44. Yi,R., O'Carroll,D., Pasolli,H.A., Zhang,Z., Dietrich,F.S., Tarakhovsky,A. and Fuchs,E. (2006) Morphogenesis in skin is governed by discrete sets of differentially expressed microRNAs. *Nat. Genet.*, **38**, 356–362.
45. Lewandoski,M., Wassarman,K.M. and Martin,G.R. (1997) Zp3-cre, a transgenic mouse line for the activation or inactivation of loxP-flanked target genes specifically in the female germ line. *Curr. Biol.*, **7**, 148–151.
46. Griffiths-Jones,S. (2004) The microRNA Registry. *Nucleic Acids Res.*, **32**, D109–D111.
47. Griffiths-Jones,S., Grocock,R.J., van Dongen,S., Bateman,A. and Enright,A.J. (2006) miRBase: microRNA sequences, targets and gene nomenclature. *Nucleic Acids Res.*, **34**, D140–D144.
48. Griffiths-Jones,S., Saini,H.K., van Dongen,S. and Enright,A.J. (2008) miRBase: tools for microRNA genomics. *Nucleic Acids Res.*, **36**, D154–D158.
49. Kozomara,A. and Griffiths-Jones,S. (2011) miRBase: integrating microRNA annotation and deep-sequencing data. *Nucleic Acids Res.*, **39**, D152–D157.
50. Kozomara,A. and Griffiths-Jones,S. (2014) miRBase: annotating high confidence microRNAs using deep sequencing data. *Nucleic Acids Res.*, **42**, D68–D73.
51. Kent,W.J., Sugnet,C.W., Furey,T.S., Roskin,K.M., Pringle,T.H., Zahler,A.M. and Haussler,D. (2002) The human genome browser at UCSC. *Genome Res.*, **12**, 996–1006.
52. Langmead,B., Trapnell,C., Pop,M. and Salzberg,S.L. (2009) Ultrafast and memory-efficient alignment of short DNA sequences to the human genome. *Genome Biol.*, **10**, R25.
53. Jurka,J. (2000) Repbase update: a database and an electronic journal of repetitive elements. *Trends Genet.*, **16**, 418–420.
54. García-López,J., Hourcade,J.e.D., Alonso,L., Cárdenas,D.B. and del Mazo,J. (2014) Global characterization and target identification of piRNAs and endo-siRNAs in mouse gametes and zygotes. *Biochim. Biophys. Acta.*, **1839**, 463–475.
55. Kuramochi-Miyagawa,S., Kimura,T., Yomogida,K., Kuroiwa,A., Tadokoro,Y., Fujita,Y., Sato,M., Matsuda,Y. and Nakano,T. (2001) Two mouse piwi-related genes: miwi and mili. *Mech. Dev.*, **108**, 121–133.
56. Ding,X., Guan,H. and Li,H. (2013) Characterization of a piRNA binding protein Miwi in mouse oocytes. *Theriogenology*, **79**, 610–615.
57. Veselovska,L., Smallwood,S.A., Saadeh,H., Stewart,K.R., Krueger,F., Maupetit-Méhouas,S., Arnaud,P., Tomizawa,S., Andrews,S. and Kelsey,G. (2015) Deep sequencing and de novo assembly of the mouse oocyte transcriptome define the contribution of transcription to the DNA methylation landscape. *Genome Biol.*, **16**, 209.
58. Meikar,O., Da Ros,M., Korhonen,H. and Kotaja,N. (2011) Chromatoid body and small RNAs in male germ cells. *Reproduction*, **142**, 195–209.
59. Nguyen-Chi,M. and Morello,D. (2011) RNA-binding proteins, RNA granules, and gametes: is unity strength? *Reproduction*, **142**, 803–817.
60. Pillai,R.S. and Chuma,S. (2012) piRNAs and their involvement in male germline development in mice. *Dev. Growth Differ.*, **54**, 78–92.
61. Kuramochi-Miyagawa,S., Watanabe,T., Gotoh,K., Takamatsu,K., Chuma,S., Kojima-Kita,K., Shiromoto,Y., Asada,N., Toyoda,A., Fujiyama,A. *et al.* (2010) MVH in piRNA processing and gene silencing of retrotransposons. *Genes Dev.*, **24**, 887–892.
62. Vagin,V.V., Sigova,A., Li,C., Seitz,H., Gvozdev,V. and Zamore,P.D. (2006) A distinct small RNA pathway silences selfish genetic elements in the germline. *Science*, **313**, 320–324.
63. Kirino,Y. and Mourelatos,Z. (2007) Mouse Piwi-interacting RNAs are 2′-O-methylated at their 3′ termini. *Nat. Struct. Mol. Biol.*, **14**, 347–348.
64. Ohara,T., Sakaguchi,Y., Suzuki,T., Ueda,H. and Miyauchi,K. (2007) The 3′ termini of mouse Piwi-interacting RNAs are 2′-O-methylated. *Nat. Struct. Mol. Biol.*, **14**, 349–350.
65. Roovers,E.F., Rosenkranz,D., Mahdipour,M., Han,C.T., He,N., Chuva de Sousa Lopes,S.M., van der Westerlaken,L.A., Zischler,H., Butter,F., Roelen,B.A. *et al.* (2015) Piwi proteins and piRNAs in mammalian oocytes and early embryos. *Cell Rep.*, **10**, 2069–2082.

66. Brennecke,J., Aravin,A.A., Stark,A., Dus,M., Kellis,M., Sachidanandam,R. and Hannon,G.J. (2007) Discrete small RNA-generating loci as master regulators of transposon activity in Drosophila. *Cell*, **128**, 1089–1103.
67. Gunawardane,L.S., Saito,K., Nishida,K.M., Miyoshi,K., Kawamura,Y., Nagami,T., Siomi,H. and Siomi,M.C. (2007) A slicer-mediated mechanism for repeat-associated siRNA 5′ end formation in Drosophila. *Science*, **315**, 1587–1590.
68. Vourekas,A., Zheng,Q., Alexiou,P., Maragkakis,M., Kirino,Y., Gregory,B.D. and Mourelatos,Z. (2012) Mili and Miwi target RNA repertoire reveals piRNA biogenesis and function of Miwi in spermiogenesis. *Nat. Struct. Mol. Biol.*, **19**, 773–781.
69. Elbashir,S.M., Lendeckel,W. and Tuschl,T. (2001) RNA interference is mediated by 21- and 22-nucleotide RNAs. *Genes Dev.*, **15**, 188–200.
70. Blaszczyk,J., Tropea,J.E., Bubunenko,M., Routzahn,K.M., Waugh,D.S., Court,D.L. and Ji,X. (2001) Crystallographic and modeling studies of RNase III suggest a mechanism for double-stranded RNA cleavage. *Structure*, **9**, 1225–1236.
71. Zhang,H., Kolb,F.A., Jaskiewicz,L., Westhof,E. and Filipowicz,W. (2004) Single processing center models for human Dicer and bacterial RNase III. *Cell*, **118**, 57–68.
72. Watanabe,T., Cheng,E.C., Zhong,M. and Lin,H. (2015) Retrotransposons and pseudogenes regulate mRNAs and lncRNAs via the piRNA pathway in the germline. *Genome Res.*, **25**, 368–380.
73. Malki,S., van der Heijden,G.W., O'Donnell,K.A., Martin,S.L. and Bortvin,A. (2014) A role for retrotransposon LINE-1 in fetal oocyte attrition in mice. *Dev. Cell*, **29**, 521–533.
74. Olovnikov,I., Ryazansky,S., Shpiz,S., Lavrov,S., Abramov,Y., Vaury,C., Jensen,S. and Kalmykova,A. (2013) De novo piRNA cluster formation in the Drosophila germ line triggered by transgenes containing a transcribed transposon fragment. *Nucleic Acids Res.*, **41**, 5757–5768.
75. Li,C., Vagin,V.V., Lee,S., Xu,J., Ma,S., Xi,H., Seitz,H., Horwich,M.D., Syrzycka,M., Honda,B.M. *et al.* (2009) Collapse of germline piRNAs in the absence of Argonaute3 reveals somatic piRNAs in flies. *Cell*, **137**, 509–521.
76. Khurana,J.S., Xu,J., Weng,Z. and Theurkauf,W.E. (2010) Distinct functions for the Drosophila piRNA pathway in genome maintenance and telomere protection. *PLoS Genet.*, **6**, e1001246.